Scien. Tech. Bull-Chem. Food Sci. Eng., Vol. 22(XXIII), 2025, 3-17
doi: 10.62591/Scien.Tech.Bull-Chem.FoodSci.Eng.2025.22.01

Article

CHARACTERIZATION BY FTIR-ATR SPECTROSCOPY OF PM10 AND PM2.5 ATMOSPHERIC PARTICLES IN ARAD (ROMANIA) IN NORMAL PERIODS AND IN EPISODES OF SAHARAN DUST

Andreea-Corina MARCU[1], Andreea Ioana LUPITU[2], Cristian MOISĂ[2], Dorina Rodica CHAMBRE[1]*

[1]Faculty of Food Engineering, Tourism and Environmental Protection, "Aurel Vlaicu" University of Arad, 2 Elena Drăgoi, Arad 310330, Romania
[2] Interdisciplinary Research Institute of the "Aurel Vlaicu" University of Arad, 2 Elena Drăgoi, Arad 310330, Romania
Corresponding author email: dorinachambree@yahoo.com

Abstract: *Atmospheric particulate matter (PM) represents one of the most important air quality indicators due to its significant impact on human health and the environment. FTIR-ATR spectroscopy was employed to investigate the chemical composition of PM10 and PM2.5 aerosols collected at three air quality monitoring stations in Arad County, representative of urban traffic, industrial activities, urban background, and suburban environments, during both normal atmospheric conditions and Saharan dust intrusion events. Variations in filter characteristics and FTIR-ATR spectral features reflected the combined effects of seasonal conditions, local emission sources, and Saharan dust transport. The identified absorption bands corresponding to O–H, C–H, C=O, NO_3^-, CO_3^{2-}, SO_4^{2-}, and Si–O functional groups indicated the presence of both natural and anthropogenic aerosol components. The natural fraction was dominated by silicates, aluminosilicates, quartz, hydrated clay minerals, and carbonates, whereas the anthropogenic fraction included carbonaceous compounds, hydrocarbons, and secondary aerosols such as nitrates and sulfates. Enhanced mineral signatures during Saharan dust episodes confirmed the contribution of long-range transported mineral aerosols rich in illite, smectite, palygorskite, calcite, and dolomite to PM composition. The FTIR-ATR findings demonstrate the combined influence of local emissions, seasonal variability, and Saharan dust transport on particulate matter composition in western Romania.*

Keywords: PM10 and PM2.5; FTIR-ATR spectroscopy; chemical composition; aerosol characterization; Saharan dust intrusion.

INTRODUCTION

Air pollution is one of the major environmental challenges of the 21st century, with significant impacts on human health, ecosystems, and climate. Among air pollutants, particulate matter (PM) is considered a key indicator of air quality due to its ability to penetrate the respiratory system and transport various chemical contaminants (Ofremu et al., 2025; Taha et al., 2025). Atmospheric particles are classified according to their aerodynamic diameter, with PM10 and PM2.5 representing the fractions of greatest relevance for air quality and health assessments.

The health effects of particulate matter depend on both particle size and chemical composition. PM10 particles are mainly deposited in the upper respiratory tract, whereas PM2.5 particles can reach the pulmonary alveoli and enter the bloodstream (Ofremu et al., 2025; Taha et al., 2025, Hamanaka and Mutlu, 2025). Numerous epidemiological studies have linked long-term PM exposure to respiratory and cardiovascular diseases and increased premature mortality (Ofremu et al., 2025; Taha et al., 2025). Consequently, the World Health Organization (WHO) and the European Union have established air quality standards and guideline values for PM10 and PM2.5 concentrations (WHO, 2025; WHO, 2024). Effective monitoring systems and continuous air quality assessment programs are therefore essential for identifying pollution episodes and supporting public health protection measures (EEA, 2024).

Atmospheric particulate matter consists of a complex mixture of organic and inorganic

compounds, including sulfates, nitrates, ammonium salts, elemental carbon, organic matter, trace metals, metalloids, and mineral particles (Seinfeld and Pandis, 2016; Romano et al., 2022). Its composition is influenced by emission sources, meteorological conditions, and atmospheric transport and transformation processes, making PM characterization an important tool for source identification and environmental impact assessment (Harrison and Hester, 2009; Shankar et al., 2022; Mohandoss et al., 2025).

In Central Europe, PM10 and PM2.5 originate from both anthropogenic sources, such as traffic, industry, energy production, residential heating, and agriculture, and natural sources, including soil dust resuspension, wildfires, and long-range transport of mineral aerosols (EEA, 2025; EEA, 2024). Recent studies have highlighted the significant contribution of transboundary pollution to particulate matter levels across Europe (Velásquez-García et al., 2024; Oduber et al., 2026; Basart et al., 2023).

Particular attention has been given to Saharan dust transport events, during which large quantities of mineral aerosols originating from North Africa reach the Mediterranean Basin and subsequently Central and Eastern Europe. These episodes can substantially increase PM10 concentrations and modify aerosol composition and atmospheric optical properties (Querol et al., 2009; Gkikas et al., 2021; Varrica et al., 2019). Recent studies indicate an increasing frequency and intensity of Saharan dust intrusions, affecting regions located hundreds or even thousands of kilometers from the source areas (Rodríguez et al., 2024; Varga, 2023).

Arad County, located along Romania's western border, is among the first regions affected by air masses originating from southwestern Europe. Its position on major European transport corridors and its proximity to important industrial and urban areas in Romania and Hungary expose the region to both local and transboundary sources of air pollution. Consequently, during Saharan dust intrusion events, Arad is often among the first areas in Romania to experience increased particulate matter concentrations due to the prevailing southwesterly air mass circulation (https://apmar.anpm.ro).

The municipality of Arad represents the main urban and economic center of the county, characterized by intense road traffic, industrial and logistics activities, and a high population density. Major emission sources include traffic along the E68 and E671 European corridors, urban traffic, activities within the Arad-West industrial area, and centralized and residential heating systems, particularly during the cold season. In addition, the topographic characteristics of the Western Plain may favor the temporary accumulation of pollutants under stable atmospheric conditions.

Air quality monitoring is performed through automatic stations integrated into the National Air Quality Monitoring Network (RNMCA), managed by the Arad Environmental Protection Agency (DJM Arad) (https://anmap.gov.ro/reteaua-nationala-de-monitorizare-automata-a-calitatii-aerului-rnmca/). In Arad County, monitoring is carried out at two stations located in the municipality of Arad (AR1 and AR2) and one station in the Nădlac area (AR3), providing continuous data on major atmospheric pollutants. These measurements support air quality assessment, the identification of pollution episodes, and studies on atmospheric aerosol dynamics and population exposure to air pollutants. The AR1 monitoring station is situated in an urban area characterized by intense road traffic and industrial activities, including emissions associated with the CET-H electrothermal power plant, and is representative of pollution generated by these sources. The AR2 station is located within a residential area and is considered representative of the urban background conditions of Arad. In contrast, the AR3 station is situated near the Nădlac border crossing with Hungary and is representative of the combined influence of international road traffic and the resuspension of mineral particles from surrounding agricultural land and transportation corridors.

PM10 and PM2.5 samples were collected in accordance with the SR EN 12341 standard using automatic samplers equipped with size-selective inlets for the retention of particles with aerodynamic diameters below 10

μm and 2.5 μm, respectively (https://www.mmediu.ro/app/webroot/uploads/files/Ghid%20G1.pdf). Particles were collected on quartz fiber filters during 24-hour sampling periods under controlled operating conditions. PM concentrations were determined gravimetrically following filter conditioning and weighing procedures specified by the standard. After analysis, the filters were individually sealed and stored under controlled temperature and humidity conditions to preserve their physicochemical properties.

The characterization of atmospheric particulate matter is essential for identifying emission sources and understanding aerosol transport and transformation processes. Among the available analytical techniques, FTIR-ATR spectroscopy has proven particularly useful for investigating the chemical composition of atmospheric particles, while complementary methods such as ICP-MS and SEM-EDS provide additional information on elemental composition and particle morphology (Varrica et al., 2019; Gupta et al., 2024; Radulescu et al., 2017).

FTIR-ATR enables the identification of functional groups and major chemical constituents in particulate matter using small sample quantities and minimal preparation (Radulescu et al., 2017; Mahmud et al., 2024; Maria et al., 2002; Coury and Dillner, 2008; Russell, 2003). Its rapid and non-destructive nature allows the simultaneous characterization of both organic and inorganic aerosol components, making it a valuable tool for atmospheric particle analysis.

The aim of this study was to characterize the chemical composition of PM10 and PM2.5 atmospheric particles collected at different air quality monitoring sites in Arad County, Romania, using ATR-FTIR spectroscopy, with a focus on assessing the influence of local emission sources, seasonal variability, and Saharan dust intrusion events on the chemical characteristics of atmospheric aerosols.

MATERIALS AND METHODS

Material:

This study was based on the analysis of PM10 and PM2.5 particulate matter samples collected on quartz fiber filters and selected from the archive of the Chemical Analysis Laboratory of the DJM Arad. The filters were obtained through routine monitoring activities carried out within the National Air Quality Monitoring Network (RNMCA) at the three automatic air quality monitoring stations AR1, AR2, and AR3.The sampling periods corresponding to the investigated filter samples are presented in Table 1, whereas Table 2 summarizes the coding mode. Figure 1 shows the PM10 and PM2.5 filter samples selected for FTIR-ATR analysis

Table 1. Sampling periods of the investigated filters

Sampling period	Type of samples
February 2025	PM10
March 2025	PM10 and PM2.5
July 2025	PM10
24–25 March 2025	PM10 –episode of Saharan dust
March 2018	PM10
April 17–18, 2018	PM10 –episode of Saharan dust

Table 2. Sample identification codes

Sample code	Date	Filter	Saharan dust **(PS)**
AR1 Location			
AR1-25-1	20.02.2025	PM10	NO
AR1-25-2	20.03.2025	PM10	NO
AR1-25-3	27.07.2025	PM10	NO
AR1-25-PS	24.03.2025	PM10	YES
AR1-18-1	16.03.2018	PM10	NO
AR1-18-PS	17.04.2018	PM10	YES
AR2 Location			
AR2-25-1	20.03.2025	PM10	NO
AR2-25-2	20.03.2025	PM2,5	NO
AR2-25-3	27.07.2025	PM10	NO
AR2-25-PS	24.03.2025	PM10	YES
AR2-18-PS	17.04.2018	PM10	YES
AR3 Location			
AR3-25-1	19.03.2025	PM10	NO
AR3-25-2	20.03.2025	PM10	NO
AR3-25-3	27.07.2025	PM10	NO
AR3-25-PS	24.03.2025	PM10	YES
AR3-18-PS	17.04.2018	PM10	YES

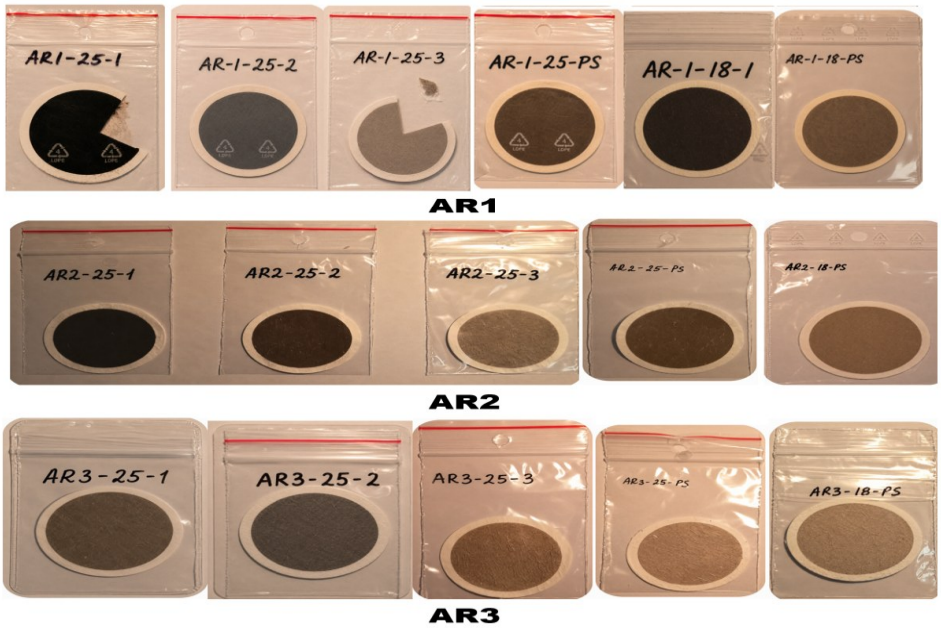

Figure 1. Filter sample images.

Method:

Prior to spectroscopic analysis, the filters were visually examined using a magnifying glass in order to evaluate their general appearance, coloration, surface texture, particle distribution, and particulate matter loading.

For FTIR-ATR analysis, representative fragments were collected from the particulate matter-loaded regions of each filter. The surface layer containing the deposited atmospheric particles was carefully isolated from the filter substrate using stainless-steel tweezers and subsequently used for spectral acquisition.

FTIR-ATR analyses were performed using a Vertex 70 spectrometer (Bruker, Germany) equipped with a ZnSe ATR crystal. Spectra were recorded in the 4000–600 cm^{-1} and 1900–600 cm^{-1} ranges at a resolution of 4 cm^{-1}, with 64 scans accumulated for each measurement. Representative fragments from the particulate matter-loaded areas of the filters were placed directly onto the ATR crystal. Prior to each analysis, a background spectrum was recorded using an unexposed portion of the same filter material to compensate for spectral contributions from the filter substrate. The ATR crystal was cleaned with isopropyl alcohol between successive measurements to prevent cross-contamination. Spectral acquisition and processing, including baseline correction, were performed using OPUS 6.3 software (Bruker). For each sample, three replicate measurements were carried out, and the results are presented as the average spectrum.

RESULTS AND DISCUSSIONS

According to Law No. 104/2011 on ambient air quality, the limit value for PM10 is 50 µg m^{-3} as a daily average, with no more than 35 exceedances permitted per year, and 40 µg m^{-3} as an annual average. For PM2.5, the annual limit value is 25 µg m^{-3}.
(http://www.calitateaer.ro/export/sites/default/.galleries/Legislation/national/Lege-nr.-104_2011-calitatea-aerului-inconjurator.pdf)

Table 3 summarizes the PM10 and PM2.5 concentrations determined by the gravimetric method for the analyzed filter samples collected over a 24-hour sampling period and identifies the instances in which the regulatory limit values were exceeded.

Table 3. Gravimetric PM values for filter samples (DJM Arad, Chemical Analysis Laboratory)

Sample code	PM value (µg/m³)	PM10 limit value exceeded (50 µg/m³)
AR1-25-1	55	YES
AR1-25-2	47	NO
AR1-25-3	26	NO
AR1-25-PS	61	YES
AR1-18-1	34	NO
AR1-18-PS	65	YES
AR2-25-1	51	YES

AR2-25-2	17	NO *
AR2-25-3	22	NO
AR2-25-PS	60	YES
AR2-18-PS	63	YES
AR3-25-1	32	NO
AR3-25-2	35	NO
AR3-25-3	21	NO
AR3-25-PS	68	YES
AR3-18-PS	72	YES

* For PM2.5 there is no daily limit value in the Romanian legislation; The comparison is made only as a guideline against the annual limit value of 25 μg/m³.

The PM concentrations revealed variations among the three monitoring sites (AR1, AR2, and AR3), as well as between normal atmospheric conditions and Saharan dust intrusion events. The highest PM10 concentrations were recorded during Saharan dust episodes, frequently exceeding the daily limit value of 50 μg m^{-3} established by national legislation. Maximum values were observed for samples AR3-18-PS (72 μg m^{-3}), AR3-25-PS (68 μg m^{-3}), and AR1-18-PS (65 μg m^{-3}), highlighting the significant contribution of long-range transported mineral aerosols.

Among the investigated sites, AR1, influenced by both road traffic and industrial activities, generally exhibited the highest particulate matter concentrations, with PM10 values ranging from 26 to 55 μg m^{-3} under non-Saharan conditions. In contrast, AR2, representative of the urban background environment, recorded lower concentrations, reflecting a reduced influence of local anthropogenic sources. The substantial difference between samples AR2-25-1 (PM10 = 51 μg m^{-3}) and AR2-25-2 (PM2.5 = 17 μg m^{-3}), collected on the same day, indicates a significant contribution of coarse particles (2.5–10 μm) to the total aerosol burden. AR3, showed intermediate concentration levels influenced by both traffic emissions and the resuspension of mineral particles from surrounding open areas.

Lower particulate matter concentrations were generally recorded during the summer period, with PM10 values decreasing to approximately 21 μg m^{-3}. Overall, 8 of the 16 analyzed samples exceeded the daily PM10 limit value, most of them being associated with Saharan dust intrusion events. However, exceedances were also observed under non-Saharan conditions at sites strongly affected by road traffic.

These findings demonstrate the combined influence of local anthropogenic emissions and long-range transport of mineral aerosols on particulate matter levels in the Arad region.

Preliminary characterization of the filtres

During the warm season, atmospheric mineral particle concentrations generally increase due to soil drying, road dust resuspension, agricultural activities, and construction work (Harrison and Hester, 2009; Amato, 2018). In addition, Saharan dust intrusion events occur more frequently during spring and summer. Consequently, PM10 filters typically exhibit light gray to brownish shades associated with mineral deposits (Querol et al., 2009).

During Saharan dust events, the filters often display yellowish-brown, reddish-brown, or grayish-brown coloration due to the increased contribution of mineral particles rich in silicates, carbonates, and iron oxides transported from North Africa (Seinfeld and Pandis, 2016; Querol et al., 2009).

In the cold season, high soil moisture and snow cover reduce the resuspension of mineral particles, while emissions from residential heating and road traffic increase, leading to a greater contribution of combustion-derived compounds (Basart et al., 2023; Gkikas et al., 2021). Consequently, PM10 filters collected during winter generally exhibit darker shades, ranging from dark gray to black, reflecting the increased presence of elemental carbon.

The visual examination of the PM10 and PM2.5 filters (Fig.1) revealed noticeable differences in coloration and particle loading depending on the season, sampling location, and the occurrence of Saharan dust intrusion events. Filters collected during the cold season generally exhibited dark gray to black coloration and a high degree of particle loading, reflecting the increased contribution of carbonaceous aerosols associated with road traffic, residential heating, and other combustion processes. In contrast, filters collected during the warm season showed lighter gray, beige, or brownish shades, indicating a greater contribution of mineral particles originating from road dust

resuspension, agricultural activities, and other natural sources. Samples associated with Saharan dust intrusion events were characterized by grayish-brown, beige-brown, or reddish-brown coloration. Differences were also observed among the monitoring sites, with filters collected in areas strongly influenced by traffic and anthropogenic activities displaying darker coloration and higher particle loading than those collected in locations with a greater contribution of mineral dust. Overall, the visual characteristics of the filters reflected the combined effects of seasonal conditions, local emission sources, and Saharan dust transport on the composition of atmospheric particulate matter.

Interpretation of FTIR-ATR spectra

In recent years, Fourier Transform Infrared Spectroscopy (FTIR) has become an important tool for the characterization of atmospheric aerosols, enabling the identification of both organic and inorganic constituents of particulate matter (Romano et al., 2022; Shankar et al., 2022; Varrica et al., 2019). The combination of FTIR with Attenuated Total Reflectance (ATR) significantly expands its applicability to solid samples, allowing rapid, non-destructive analysis with minimal sample preparation (Mohandoss et al., 2025; Gupta et al., 2024; Mahmud et al., 2024). The study published by Varrica D. et al. (Varrica et al., 2019) demonstrates that ATR-FTIR analysis can be successfully used for the chemical characterization of PM10 and PM2.5 and for highlighting the influence of Saharan dust episodes on the composition and concentration of atmospheric particles.

Figures 2–4 show the FTIR-ATR spectra of the PM10 samples collected on 20 March 2025 at the AR1, AR2, and AR3 monitoring stations, whereas Table 4 presents the vibrational assignments of the principal absorption bands observed in the recorded spectra.

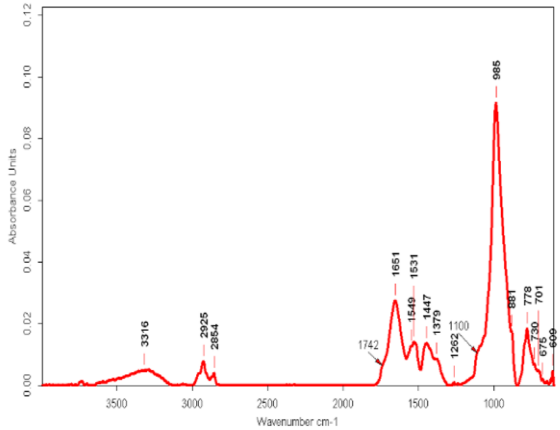

Figure 2. FTIR-ATR spectrum of sample **AR1-25-2**

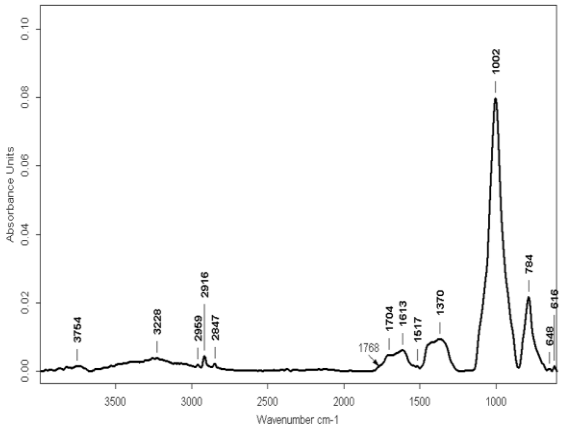

Figure 3. FTIR-ATR spectrum of sample **AR2-25-1**

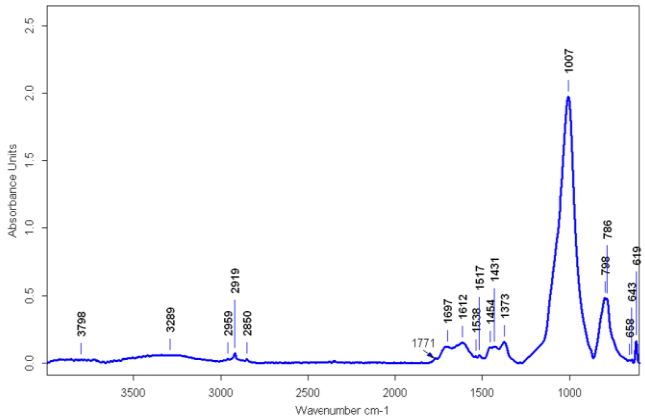

Figure 4. FTIR-ATR spectrum of the **AR3-25-2 sample**

Table 4. Vibrational assignment of FTIR-ATR bands for PM10 samples collected on 20.03.2025

Wavenumber (cm^{-1})	AR1-25-2	AR2-25-1	AR3-25-2	Vibrational assignment	Probable compounds	Ref.
~3800–3200	3316	3754, 3228	3798, 3289	ν(O–H) stretching	Adsorbed water, hydroxyl groups of clays, silicates and hydrated minerals	(Coury and Dillner, 2008; Gupta et al., 2024; Mahmud et al., 2024; Maria et al., 2002; Mohandoss et al., 2025; Romano et al., 2022; Russell, 2003; Shankar et al., 2022; Varrica et al., 2019)
~2960–2915	2925	2959, 2916	2959, 2919	ν as(C–H)	Aliphatic hydrocarbons, carbonaceous compounds from traffic and combustion	
~2855–2845	2854	2847	2850	νs(C–H)	Aliphatic chains of hydrocarbons	
~1775–1690	1742	1768, 1704	1771, 1697	ν(C=O) stretching	Esters, aldehydes, ketones, carboxylic acids and secondary organic aerosols	
~1655–1600	1651	1613	1612	δ(H–O–H), ν(C=C)	Adsorbed water, oxidized organic matter, aromatic compounds	
~1550–1500	1549, 1531	1517	1538, 1517	$\nu(NO_3^-)$, ν(C=C) aromatic	Nitrates and aromatic compounds	
~1455–1370	1447, 1373	1370	1454, 1431, 1373	$\nu_3(CO_3^{2-})$, $\delta(CH_3)$	Carbonates (calcite, dolomite), organic matter	
~1265–1100	1262, 1100	–	–	ν (C–O), ν (SO_4^{2-})	organic compounds Secondary sulphates	
~1030–980	985	1002	1007	ν(Si–O–Si), ν(Si–O)	Quartz, silicates, aluminosilicates, clays	
~800–770	778	784	798, 786	ν(Si–O)	Quartz and crystalline silicates	
~700–560	701, 675, 609	648, 616	643, 619, 568	δ(Si–O), Al–O–Si	Aluminosilicates, clays, feldspars	

The FTIR-ATR spectra of samples AR1-25-2, AR2-25-1, and AR3-25-2 (Figs. 2–4) exhibit similar spectral features, indicating the presence of both organic and inorganic constituents typical of atmospheric aerosols. The identified absorption bands suggest that PM10 particles collected at the three monitoring stations consist of a complex mixture of mineral phases, including silicates, quartz, aluminosilicates, and carbonates, together with organic compounds originating from combustion processes and secondary atmospheric transformations. These findings are consistent with previous studies on the chemical composition of atmospheric particulate matter (Romano et al., 2022; Shankar et al., 2022; Varrica et al., 2019; Gupta et al., 2024). The observed differences among the samples reflect the influence of local emission sources and site-specific conditions, with a more pronounced mineral contribution in sample AR3-25-2 and a stronger anthropogenic influence in samples AR1-25-2 and AR2-25-1.

The most intense absorption band, observed in the 986–1007 cm^{-1} region, represents the dominant spectral feature of all analyzed samples. Although the sampling filters are composed of quartz fibers, their spectral contribution was compensated by recording the background spectrum using an unexposed

portion of the same filter material. As illustrated in Fig. 5, the quartz fiber filter exhibits characteristic absorption bands at approximately 1027 and 802 cm^{-1}; however, these bands are effectively removed during background correction. Consequently, the remaining absorption band in the 986–1007 cm^{-1} region can be attributed to particulate matter deposited on the filters, indicating a significant contribution of silicate-rich mineral particles.

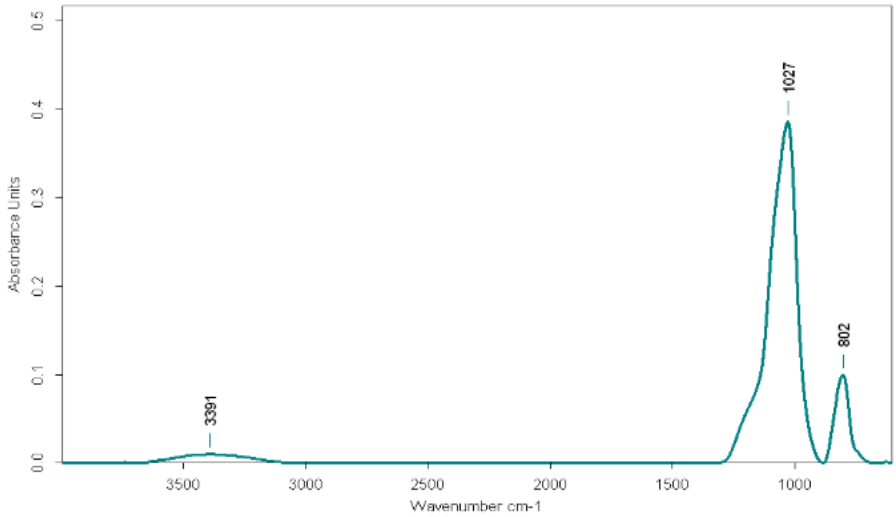

Figure 5. FTIR-ATR Spectrum of quartz fiber filter

Table 5. Comparison of PM10 samples collected on 20.03.2025

Parameter	AR1-25-2	AR2-25-1	AR3-25-2
Station type	Traffic and Industrial	Urban Background	Suburban Traffic
PM10 (μg m^{-3})	47	51	35
Dominant absorption band (cm^{-1})	985	1002	1007
Organic signature (C–H, C=O)	Pronounced	Pronounced	Moderate
Nitrates Secondary aerosols	Pronounced	Moderate	Pronounced
Carbonates	Moderate	Weak	Pronounced
Silicates and alumino-silicates	High	High	Very high
Predominant pollution sources	Traffic and industry	Mixed urban background	Resuspended mineral particles and traffic

In all three spectra, a broad band at 3800–3200 cm^{-1} is attributed to O–H stretching vibrations associated with hydroxyl groups and adsorbed water (Mohandoss et al., 2025; Varrica et al., 2019; Rodríguez et al., 2024). Bands in the 2960–2850 cm^{-1} region correspond to C–H stretching vibrations of aliphatic hydrocarbons, indicating contributions from combustion processes and road traffic (Shankar et al., 2022; Varrica et al., 2019). Absorption bands between 1770 and 1600 cm^{-1} are associated with carbonyl (C=O) groups and oxygenated organic compounds, suggesting the presence of secondary organic aerosols (Romano et al., 2022; Mohandoss et al., 2025; Maria et al., 2002), while bands at 1550–1500 cm^{-1} indicate nitrates and other secondary inorganic species (Coury and Dillner, 2008; Russell, 2003). The most intense bands, observed in the 1030–980 cm^{-1} region, are attributed to Si–O–Si and Si–O vibrations characteristic of silicates, quartz, and aluminosilicates (Varrica et al., 2019; Coury and Dillner, 2008). Together with the bands detected at 800–600 cm^{-1}, they confirm a significant contribution of mineral particles derived from crustal materials and soil dust resuspension. The bands in the 1455–1370 cm^{-1} range, assigned to CO_3^{2-} asymmetric stretching vibrations, indicate the presence of carbonate minerals such as calcite and dolomite (Varrica et al., 2019; Russell, 2003). Among the analyzed samples, AR3-25-2 exhibited the strongest mineral signature, evidenced by the higher intensity of silicate- and carbonate-related bands, whereas AR1-25-2 and AR2-25-1 showed a relatively

greater contribution of organic compounds and secondary aerosols associated with anthropogenic activities (Mohandoss et al., 2025; Gupta et al., 2024; Mahmud et al., 2024; Romano et al., 2022). These findings are consistent with the gravimetrically determined PM10 concentrations and the characteristics of the monitoring sites summarized in Table5.

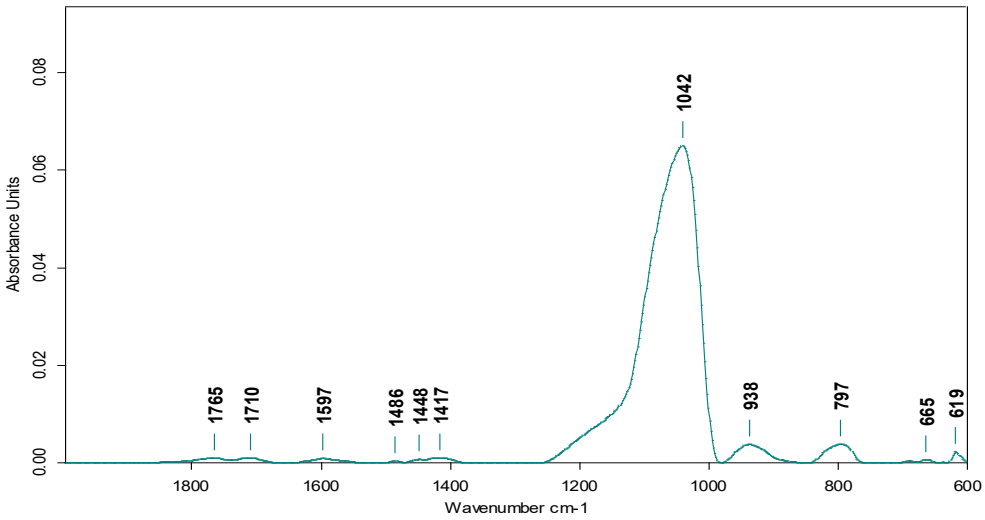

Figure 6. FTIR-ATR spectrum of sample **AR2-25-2 (PM2.5)**

Table 6. Vibrational assignment of FTIR-ATR bands, sample **AR2-25-2 (PM2.5)**

Wavenumber (cm^{-1})	**Vibrational assignment**	**Probable compounds**	**Ref.**
~1640–1650	δ(H–O–H), ν(C=C)	Adsorbed water, oxidized organic compounds, aromatic structures	(Coury and Dillner, 2008; Gupta et al., 2024; Mahmud et al., 2024; Maria et al., 2002; Mohandoss et al., 2025; Radulescu et al., 2017; Russell, 2003; Shankar et al., 2022; Varrica et al., 2019)
~1570–1550	ν(NO_3^-), ν(C=C) aromatic	Secondary nitrates and aromatic compounds	
~1530	ν (NO_3^-)	Inorganic nitrates and secondary aerosols	
~1460–1450	$\nu_s(CO_3^{2-})$, δ(CH_2)	Carbonates (calcite, dolomite) and organic matter	
~1420	$\nu_{as}(CO_3^{2-})$	Carbonates and carbonate compounds of mineral origin	
~1000–1010	ν(Si–O–Si), ν(Si–O)	Quartz, silicates, aluminosilicates	
~940	ν(Si–OH)	Hydrated silicates and clays	
~835	δ(Si–O)	Quartz and crystalline silicates	
~795–780	ν(Si–O)	Quartz (α-quartz)	
~620–610	δ(Si–O), Al–O–Si	Aluminosilicates and clays	

The FTIR-ATR spectrum of sample AR2-25-2 (PM2.5) is dominated by a very intense absorption band at approximately 1000–1010 cm^{-1}, attributed to Si–O–Si and Si–O stretching vibrations characteristic of silicates, aluminosilicates, and other crustal mineral particles (Varrica et al., 2019; Coury and Dillner, 2008). The high intensity of this band indicates a substantial contribution of mineral material, likely associated with soil dust resuspension and mineral aerosol transport. Several low-intensity bands observed in the 1650–1400 cm^{-1} region are assigned to oxygenated organic compounds, carbonyl groups, and secondary inorganic species such as nitrates and carbonates (Shankar et al., 2022; Mohandoss et al., 2025; Varrica et al., 2019; Gupta et al., 2024; Radulescu et al., 2017; Mahmud et al., 2024; Maria et al., 2002; Russell, 2003). Additional bands in the 800–600 cm^{-1} range further confirm the presence of quartz and aluminosilicates (Mohandoss et al., 2025; Varrica et al., 2019; Gupta et al., 2024; Mahmud et al., 2024; Coury and Dillner, 2008).

The spectra of AR2-25-1 (PM10) and AR2-25-2 (PM2.5) display a similar mineral-dominated profile, suggesting common sources of atmospheric particles at the AR2 station. However, the PM10 sample exhibits more pronounced bands associated with organic compounds and secondary aerosols, particularly at 1742, 1651, 1549, and 1531 cm^{-1}, indicating a more complex chemical composition. In contrast, the PM2.5 fraction is dominated by silicate-rich mineral particles. A similar pattern was reported by Radulescu et al. (Radulescu et al., 2017) for PM2.5 samples collected in Târgoviște.

The comparative analysis of the FTIR-ATR spectra of PM10 samples collected during the cold and warm seasons at the AR1, AR2, and AR3 monitoring stations revealed clear seasonal differences in aerosol composition (Figs. 7–9, Table 7). Samples collected during the cold season showed more pronounced bands associated with carbonyl compounds, nitrates, and secondary aerosols, reflecting the influence of combustion-related emissions and atmospheric conditions favorable to pollutant accumulation. In contrast, warm-season samples were characterized by stronger silicate- and carbonate-related bands, indicating an increased contribution of mineral particles derived from soil dust resuspension and regional dust transport.

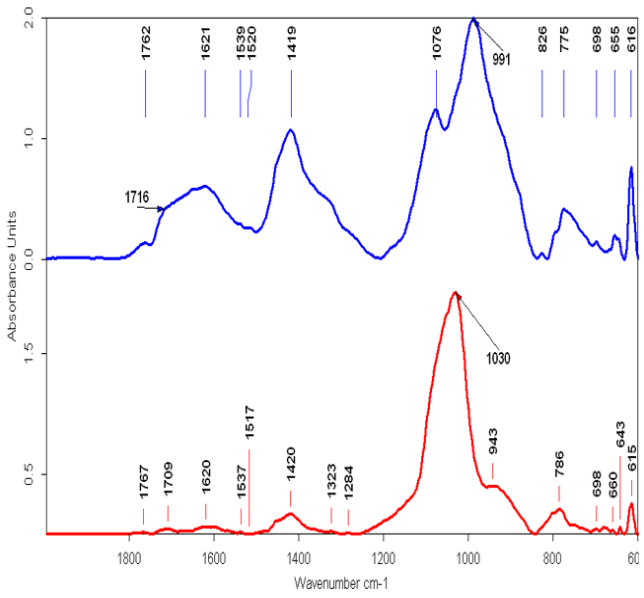

Figure 7. FTIR-ATR spectra of samples collected at AR1 station in different seasons: (____)AR1-25-1- cold season; (____)AR1-25-3 – warm season

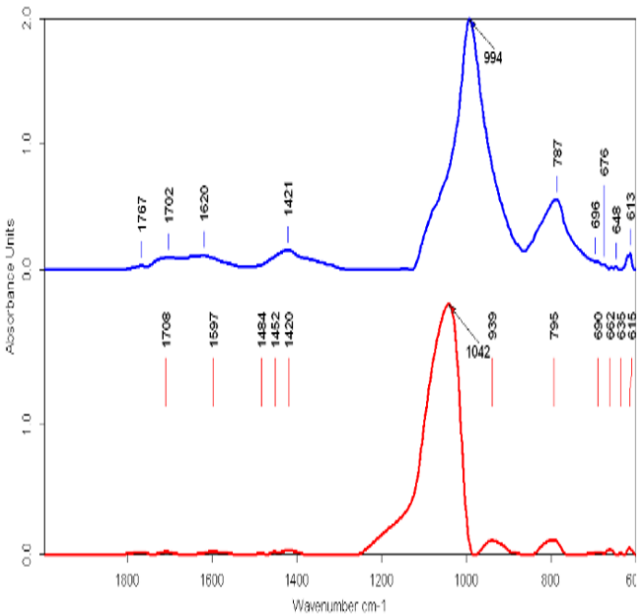

Figure 8. FTIR-ATR spectra of samples collected at AR2 station in different seasons: (____) AR2-25-1 - cold season; (____) AR2-25-3 - warm season

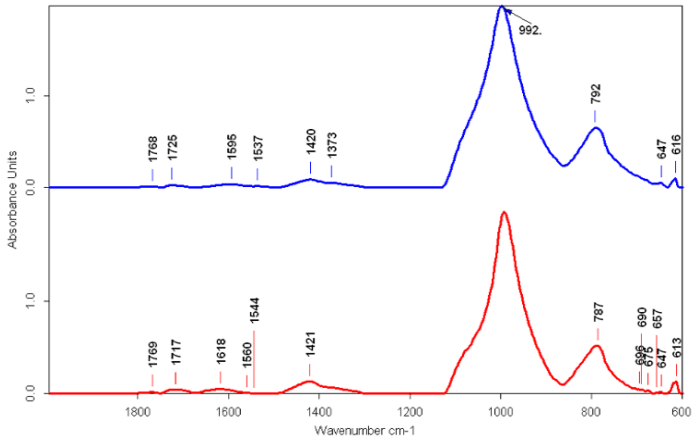

Figure 9. FTIR-ATR spectra of samples collected at AR3 station in different seasons: (____) AR3-25-1- cold season; (____) AR3-25-3 - warm season

Table 7. Comparison between stations

Feature	AR1	AR2	AR3
Difference between Cold Season and Warm Season	High	Very high	Moderate
Organic signature in the cold season	Pronounced	Pronounced	Moderate
Nitrates/secondary aerosols in the cold season	Highlights	Highlights	Highlights
Carbonates in the warm season	Moderate	Moderate	Pronounce
Silicate-mineral component in the warm season	High	Very high	Very high
Annual crustal influence	Moderate	High	Very high

Among the three monitoring stations, AR2 exhibited the greatest seasonal variability, shifting from a relatively complex aerosol composition during the cold season to a profile dominated by mineral particles during the warm season. AR1 showed a stronger influence of anthropogenic sources in the cold season, consistent with the urban and industrial characteristics of the site. In contrast, AR3 maintained the most persistent mineral signature throughout the year, indicating a continuous contribution of crustal particles and resuspended dust associated with both traffic-related and natural sources.

The Saharan dust intrusion events identified in 2018 and 2025 significantly affected air quality in the municipality of Arad, leading to elevated PM10 concentrations and an increased contribution of crustal mineral particles, as shown in Table 3. The FTIR-ATR spectra recorded during the Saharan dust intrusion events (Figs. 10 and 11) exhibited a more pronounced mineral signature than those obtained under normal atmospheric conditions. A comparison of the FTIR-ATR spectra of samples AR1-18-PS and AR1-18-1 presented in Fig. 10 reveals a broadly similar spectral fingerprint dominated by absorption bands characteristic of silicate compounds, while also exhibiting notable differences in the intensity and distribution of specific spectral features. The sample collected during the Saharan dust event (AR1-18-PS) was distinguished from the non-Saharan sample (AR1-18-1) by the presence of a distinct absorption band at approximately 1143 cm^{-1} and a pronounced enhancement of the band at 1624 cm^{-1}. The absorption band observed at 1143 cm^{-1} is associated with Si–O stretching vibrations in aluminosilicate minerals, including illite, smectite, and palygorskite, which are characteristic constituents of Saharan dust originating from Algeria, Tunisia, and Morocco (Caquineau et al.2002, Formenti et al.2011). The band at 1624 cm^{-1} is attributed to hydrated clay minerals and water adsorbed onto their surfaces (Varrica et al., 2019). In addition, the spectra exhibit a distinct absorption band at approximately 1423 cm^{-1}, assigned to carbonate minerals such as calcite and dolomite, which are frequently reported in association with illite, smectite, and palygorskite in Saharan dustransported from North Africa (Varrica et al., 2019.. The occurrence of these mineralogical markers confirms the significant contribution of long-

range transported Saharan aerosols to the PM10 composition. Similar spectral behavior during Saharan dust intrusion events was reported by Varrica et al. (Varrica et al., 2019) for atmospheric particulate matter collected in Palermo.

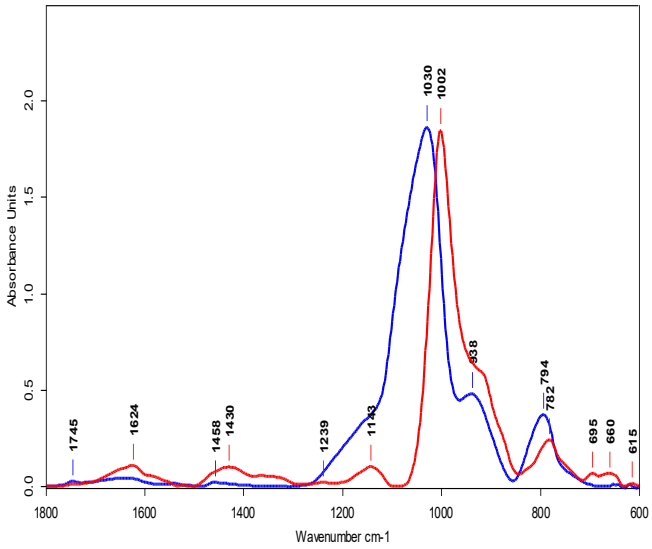

Figure 10. Comparative FTIR-ATR spectra for PM10 samples taken at the AR1 station in 2018 during an intense Saharan dust episode: (___) **AR1-18-PS**; during the normal period (___) **AR1-18-1**

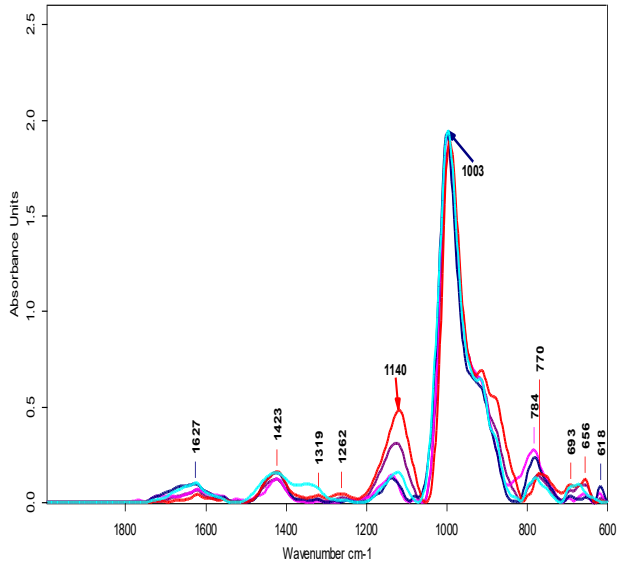

Figure 11. FTIR-ATR spectra for PM10 samples taken during periods of Saharan dust: (___) **AR3-18-PS,** (___) **AR3-25-PS**, (___) **AR1-25-PS**, (___) **AR2-25-PS**, (___) **AR2-18-PS**

Figure 11 shows a consistent FTIR-ATR spectral fingerprint for PM10 samples collected during the Saharan dust events of 2018 and 2025. All spectra are dominated by mineral absorption bands associated with silicates, aluminosilicates, and carbonates, confirming the influence of Saharan mineral aerosols on PM10 composition in Arad County.

Among the investigated sites, AR3 exhibited the highest intensity of the 1140 cm^{-1} band during both Saharan dust events, consistent with the highest PM10 concentrations recorded at this station (72 $\mu g/m^3$ in 2018 and 68 $\mu g/m^3$ in 2025; Table 3.). These results indicate a stronger impact of long-range transported Saharan dust at the AR3 site.

Limitations

This study is based exclusively on FTIR-ATR spectroscopy; therefore, mineral phases such as illite, smectite, palygorskite, calcite, and dolomite were identified from characteristic absorption bands and literature correlations only. These assignments were not independently verified by complementary techniques such as XRD, SEM-EDS, or ICP-MS. Future studies combining FTIR-ATR with these methods would provide a more reliable mineralogical and chemical characterization of atmospheric particulate matter.

CONCLUSIONS

PM10 and PM2.5 samples collected at three representative sites in Arad County were successfully characterized using FTIR-ATR spectroscopy, demonstrating the applicability of this technique for the rapid identification of major chemical components and potential aerosol sources. FTIR-ATR analysis identified characteristic absorption bands attributed to O–H, C–H, C=O, NO_3^-, CO_3^{2-}, SO_4^{2-}, and Si–O functional groups, indicating the presence of both natural and anthropogenic aerosol constituents.

The analyzed particulate matter consisted of a complex mixture of natural and anthropogenic components. The natural fraction was dominated by silicates, aluminosilicates, quartz, hydrated clay minerals, and carbonates, whereas the anthropogenic fraction included carbonaceous compounds, aliphatic and aromatic hydrocarbons, carbonyl compounds, and secondary aerosols such as nitrates and sulfates. Seasonal variations were evident,

with a greater contribution of combustion-related compounds during the cold season and enhanced mineral signatures during the warm season.

Site-specific differences reflected the influence of local emission sources. The AR1 station was predominantly affected by traffic and industrial activities, resulting in a stronger contribution of carbonaceous compounds and secondary aerosols. The AR2 site exhibited characteristics typical of an urban background environment, while the AR3 station showed a greater influence of mineral particles, indicating a stronger contribution of crustal material and Saharian dust.

Saharan dust events significantly influenced both PM10 concentrations and aerosol composition, as evidenced by the enhanced FTIR-ATR absorption bands associated with aluminosilicates, carbonates, and hydrated clay minerals. The occurrence of characteristic absorption bands consistent with illite, smectite, palygorskite (1140 cm^{-1}), calcite, and dolomite (1423 cm^{-1}) suggests the contribution of long-range transported Saharan dust from North Africa. However, these mineral phase assignments are inferred from FTIR-ATR band positions and were not independently confirmed by XRD, SEM-EDS, or ICP-MS analyses. Overall, the results highlight the combined effects of local anthropogenic emissions, seasonal variability, and long-range atmospheric transport on particulate matter composition in Arad County. FTIR-ATR spectroscopy proved to be a valuable tool for identifying the major chemical constituents of atmospheric particles and assessing the impact of Saharan dust intrusions on regional air quality.

REFERENCES

Amato, F. (Ed.), 2018. Non-Exhaust Emissions: An Urban Air Quality Problem for Public Health. Academic Press.

Basart, S., Rémy, S., Mona, L., Cornacchia, C., Benincasa, F., Karanikolas, A., Pey, J., Querol, X., 2023. Saharan dust outbreaks over Europe: Atmospheric transport, impacts on air quality and recent trends. Atmospheric Environment 301, 119690. https://doi.org/10.1016/j.atmosenv.2023.119690

Caquineau, S., Gaudichet, A., Gomes, L., Legrand, M., Papineau, F,. 2002. Mineralogy of Saharan dust transported over northwestern tropical Atlantic Ocean in relation to source regions. Journal of Geophysical Research: Atmospheres, 107(D15), 4251. https://doi.org/10.1029/2000JD000247

Coury, C., Dillner, A.M., 2008. ATR-FTIR characterization of ambient aerosol samples. Atmospheric Environment 42(23), 5923–5932. https://doi.org/10.1016/j.atmosenv.2008.03.026

European Environment Agency (EEA), 2024. Air Quality in Europe – 2024 Report. Publications Office of the European Union, Luxembourg.

European Environment Agency (EEA), 2024. Europe's Air Quality Status 2024. European Environment Agency, Copenhagen.

European Environment Agency (EEA), 2025. Particulate Matter – PM10. Air Quality Status Report 2025. European Environment Agency, Copenhagen. https:///www.eea.europa.eu/en/analysis/publications/air-quality-status-report-2025/particulate-matter

Formenti, P., Schütz, L., Balkanski, Y., Desboeufs, K., Ebert, M., Kandler, K., Petzold, A., Scheuvens, D., Weinbruch, S., & Zhang, D., 2011. Recent progress in understanding physical and chemical properties of African and Asian mineral dust. Atmospheric Chemistry and Physics, 11, 8231–8256. https://doi.org/10.5194/acp-11-8231-2011

Gkikas, A., Proestakis, E., Amiridis, V., Kazadzis, S., Koukouli, M.E., Tsekeri, A., Mihalopoulos, N., 2021. Modelling and assessment of desert dust episodes in the Mediterranean Basin and Europe. Atmospheric Chemistry and Physics 21(10), 7915–7938. https://doi.org/10.5194/acp-21-7915-2021

Gupta, S., Shankar, S., Kuniyal, J.C., et al., 2024. Identification of sources of coarse mode aerosol particles (PM10) using ATR-FTIR and SEM-EDX spectroscopy over the Himalayan Region of India. Environmental Science and

Pollution Research 31, 15788–15808. https://doi.org/10.1007/s11356-024-31973-3
Hamanaka, R.B., Mutlu, G.M., 2025. Particulate matter air pollution: Effects on the respiratory system. Journal of Clinical Investigation 135(19). https://doi.org/10.1172/JCI190560
Harrison, R.M., Hester, R.E. (Eds.), 2009. Air Quality in Urban Environments. Royal Society of Chemistry.
Mahmud, M., Mohiuddin, K.A.B., et al., 2024. Micro-characterization of indoor deposited particles using FTIR, SEM-EDS, and XRD techniques: A case study of a university campus, Bangladesh. Aerosol and Air Quality Research 24, 230236. https://doi.org/10.4209/aaqr.230236
Maria, S.F., Russell, L.M., Turpin, B.J., Porcja, R.J., 2002. FTIR measurements of functional groups and organic mass in aerosol samples. Atmospheric Environment 36(33), 5185–5196. https://doi.org/10.1016/S1352-2310(02)00627-4
Mohandoss, R., Jain, C.D., Madhavan, B.L., Madineni, V.R., 2025. Spectroscopic and chemical compositional analysis of the atmospheric aerosols in urban and rural tropical environment of southern India. Atmospheric Environment, 121431. https://doi.org/10.1016/j.atmosenv.2025.121431
Ofremu, G.O., et al., 2025. Exploring the relationship between climate change, air pollutants, and human health: A review. Environmental Challenges 18, 101086. https://doi.org/10.1016/j.envc.2024.101086
Querol, X., Pey, J., Pandolfi, M., Alastuey, A., Cusack, M., Pérez, N., Moreno, T., Mihalopoulos, N., 2009. African dust contributions to mean ambient PM10 mass levels across the Mediterranean Basin. Atmospheric Environment 43(28), 4266–4277. https://doi.org/10.1016/j.atmosenv.2009.06.013
Radulescu, C., Stihi, C., Iordache, S., Dunea, D., Dulama, I.D., 2017. Characterization of urban atmospheric PM2.5 by ATR-FTIR, ICP-MS and SEM-EDS techniques. Revista de Chimie 68(4), 805–810. https://doi.org/10.37358/RC.17.4.5557
Rodríguez, S., López-Darias, J., et al., 2024. Extreme Saharan dust events expand northward over the Atlantic and Europe, prompting record-breaking PM10 and PM2.5 episodes. Atmospheric Chemistry and Physics 24, 12031–12053. https://doi.org/10.5194/acp-24-12031-2024
Russell, L.M., 2003. Aerosol organic-mass-to-organic-carbon ratio measurements by FTIR spectroscopy. Aerosol Science and Technology 37(10), 819–828. https://doi.org/10.1080/02786820300941
Seinfeld, J.H., Pandis, S.N., 2016. Atmospheric Chemistry and Physics: From Air Pollution to Climate Change, 3rd ed. John Wiley & Sons.
Shankar, S., Gadi, R., Sharma, S.K., Mandal, T.K., 2022. Identification of carbonaceous species and FTIR profiling of PM2.5 aerosols for source estimation in Old Delhi region of India. MAPAN 37(1–3), 1–16. https://doi.org/10.1007/s12647-022-00575-0
Taha, S.S., et al., 2025. Comprehensive review of health impacts of the exposure to air pollutants: Carbon dioxide, nitrogen oxides and particulate matter. Results in Engineering, 100182. https://doi.org/10.1016/j.rineng.2025.100182
Varga, G., 2023. Increasing frequency and changing nature of Saharan dust storm events in Europe. Hungarian Geographical Bulletin 72(4), 335–352. https://doi.org/10.15201/hungeobull.72.4.2
Varrica, D., Tamburo, E., Vultaggio, M., Di Carlo, I., 2019. ATR-FTIR spectral analysis and soluble components of PM10 and PM2.5 particulate matter over the urban area of Palermo (Italy) during normal days and Saharan events. International Journal of Environmental Research and Public Health 16(14), 2507. https://doi.org/10.3390/ijerph16142507
Velásquez-García, M.P., Loria-Salazar, S.M., Alvarez-Ospina, H., 2024. Long-range transport of air pollutants increases the impact of PM2.5 on population exposure and health. Atmospheric Chemistry and Physics 24, 11497–11518. https://doi.org/10.5194/acp-24-11497-2024
World Health Organization (WHO), 2024. Ambient (outdoor) air pollution. Fact sheet.

https:///www.who.int/news-room/fact-sheets/detail/ambient-%28outdoor%29-air-quality-and-health
World Health Organization (WHO), 2025. Air pollution. https://www.who.int/health-topics/air-pollution

ACKNOWLEDGEMENTS
The authors gratefully acknowledge the Arad County Environmental Directorate (DJM Arad) for providing the PM filter samples investigated in this study.

ISSN 1582-1021
e-ISSN 2668-4764
Edited by "Aurel Vlaicu" University Publishing House, Arad, Romania

doi:10.62591/Scien.Tech.Bull-Chem.FoodSci.Eng.2024.21.01